

# Effect of Friction Stir Welding Parameters on the Microstructure and Mechanical Properties of AA2024-T4 Aluminum Alloy

Abdel-Wahab El-Morsy

Faculty of Engineering, Rabigh Branch  
King Abdulaziz University, Saudi Arabia and  
Faculty of Engineering, Helwan University  
Cairo, Egypt

Mohamed M. Ghanem

Central Metallurgical Research and  
Development Institute  
Cairo, Egypt

Haitham Bahaitham

Faculty of Engineering  
Rabigh Branch  
King Abdulaziz University  
Saudi Arabia

**Abstract**—In this work, the effects of rotational and traverse speeds on the 1.5 mm butt joint performance of friction stir welded 2024-T4 aluminum alloy sheets have been investigated. Five rotational speeds ranging from 560 to 1800 rpm and five traverse speeds ranging from 11 to 45 mm/min have been employed. The characterization of microstructure and the mechanical properties (tensile, microhardness, and bending) of the welded sheets have been studied. The results reveal that by varying the welding parameters, almost sound joints and high performance welded joints can be successfully produced at the rotational speeds of 900 rpm and 700 rpm and the traverse speed of 35 mm/min. The maximum welding performance of joints is found to be 86.3% with 900 rpm rotational speed and 35 mm/min traverse speed. The microhardness values along the cross-section of the joints show a dramatic drop in the stir zone where the lowest value reached is about 63% of the base metal due to the softening of the welded zone caused by the heat input during joining.

**Keywords**—friction stir welding; welding parameters; 2024-t4 aluminum alloy; mechanical properties

## I. INTRODUCTION

Due to many outstanding characteristics of Aluminum (Al) and its alloys, such as excellent corrosion resistance, high strength-to-weight ratio and ease of fabrication, Al-alloys are finding a wide range of application in aircrafts, ships, automobiles, storage facilities and heat exchangers building industries [1]. The utilization of Al-alloys in such industries is highly affected by their weldability factor. In order to achieve maximum joint efficiency, the Al-alloys weld joints should have exceptional levels of their mechanical properties while maintaining minimal levels of weld-defect density. The use of conventional fusion welding process in joining Al-alloys, especially the high-strength and heat-treatable ones, is considered less efficient due to the high possibility of forming hot cracks, segregation, and porosities welding defects during the fusion and solidification phases of the process [2]. In addition, the traditional welding process often leads to deterioration of mechanical properties and degradation of corrosion resistance in the joint because of phase

transformations and the dissolution of strengthening precipitates during the fusion welding process [3-4].

To eliminate the distortions, particularly in thin sheets, and the problems associated with the traditional fusion welding processes, friction stir welding (FSW) has been developed. As a solid state joining process, FSW is a promising and a viable welding technique that can produce high-quality, defect-free, and low-cost joints particularly in the joining of high-strength Al-alloys such as highly alloyed 2xxx and 7xxx series [3, 5, 6]. In addition, FSW is considered to be the most remarkable and viable welding technique for several materials such as Al-alloys [2-8], Mg-alloys [9-10], Ti-alloys [11], Ni-base alloys [12], Cu-alloys [13], and steels [14, 15]. Moreover, FSW has the possibility of creating dissimilar joints with excellent mechanical characteristics [16-17]. During FSW process, using an inappropriate level of welding parameters can cause defects in the joint and worsen its mechanical properties [18]. Thus, it is very important to choose the optimum levels of these welding parameters in order to get a weld of appropriate quality. The present study addresses the effect of traverse and rotational speeds on the quality of Al-alloys joints produced by FSW process through analyzing the microstructure and mechanical properties of 1.5 mm 2024-T4 Aluminum alloy. The mechanical properties that have been explored include microhardness distributions, bending, and tensile strength of the welded joints.

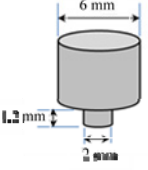
## II. EXPERIMENTAL PROCEDURE

To study the effects of rotational speed and traverse speed on the quality of friction stir butt welded joints of Al-2024-T4 Al-alloy, sheets with a thickness of 1.5 mm have been utilized. Chemical composition and mechanical properties of these sheets are presented in Table I. Using sawing machines, the sheets have been cut into 90×150×1.5 mm<sup>3</sup> strips. The FSW process has been conducted by a vertical milling machine equipped with a high-speed stirring tool, which moves perpendicular to the rolling direction. In Table II the tool geometry is illustrated along with the ranges of rotational speeds and traverse speeds applied in the FSW process.

TABLE I. CHEMICAL COMPOSITION AND MECHANICAL PROPERTIES OF AL-2024-T4

Chemical composition							
Si	Fe	Cu	Mn	Mg	Zn	Ti	Al
0.5	0.5	4.1	0.6	1.2	0.25	0.15	Bal.
Mechanical properties							
Hardness		Tensile strength			Yield stress		
160 HV		417 MPa			276 MPa		

TABLE II. WELDING PARAMETERS AND TOOL GEOMETRY

Rotational speed (rpm)	Traverse speed (mm/min)	Tool
560	35	Cylindrical pin tool geometry
700		
900		
1400		
1800		
900	11	
	18	
	28	
	35	
	45	

The joint performance has been determined by conducting optical microscopy and mechanical testing (microhardness, tensile and bend tests). The metallography samples for microstructural characterization have been taken perpendicular to the welding direction for each welded sheet. The samples have been etched using Killer's reagent base with the following chemical composition: 1.5 ml HCl, 2.5 ml HNO<sub>3</sub>, 1 ml HF and 95 ml distilled water. After being immersed for few seconds in the etching solution, the samples have been water-washed and dried in order to have them checked by the optical microscope. The hardness variation across the stirred zones of the joints has been obtained by conducting the Vickers Microhardness test on the traverse cross section of FSW samples joints. The mechanical performance of the joints has been determined through tensile testing where the ultimate tensile strength, the yield stress, and the percentage of elongation of several sets of specimens have been recorded and compared with those obtained from the base metal (BM) specimens. The specimens' sets have been prepared according to ASTM E8M-13a standard [19] where each set contains three specimens made by the predetermined settings of rotational and traverse speeds considered in the study. The bending tests have been carried out as per ASTM E290 for welded specimens to check the joints performance and weld consolidation [20-21]. For each joint, bends have been checked with mandrel diameter. In order to conduct the test, 1.5×20×180 mm<sup>3</sup> specimens have been bent around mandrel diameter 4T. The joint surface of the specimens has been examined for cracks and imperfections after reaching 180° bend by applying enough force to make the specimens' legs parallel. Figure 1 shows schematic illustration of the FSW joints and the transverse testing specimens.

### III. RESULTS AND DISCUSSION

The BM microstructure, presented in Figure 2, is mainly consisting of  $\alpha$ -solid solution of Cu-Al (the bright contrast) and secondary phases with different morphologies precipitated in the matrix (the dark contrast). As shown in the Figure, the

cladding layer of pure Al is rolled with the alloy to give high corrosion resistance by a layer of Al-oxide which cannot be penetrated by O<sub>2</sub> and prevents further attack.

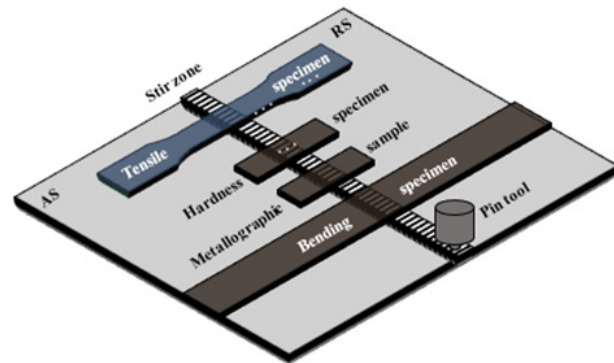


Fig. 1. Schematic illustration of the FSW and the traverse testing specimens.



Fig. 2. Optical microstructure of the base metal.

Figures 3-6 show the morphology overviews of the traverse cross sections of FSW samples at different welding conditions covering the predetermined levels of rotational and traverse speeds. In all presented cases, the joints were split into several distinct regions: BM, stir zone (SZ), heat affected zone (HAZ) and the narrow transition region which is commonly called thermo-mechanically affected zone (TMAZ). Figure 3 shows the optical micrograph of SZ at 900 rpm rotational speed and 11 mm/min traverse speed. It is observed that the clad layer has been damaged and forced into weld nugget. The indiscernible shape found in the SZ could be due to inadequate flow of metals and mixing in that zone. The improper heat applied during the FSW process has caused the void or groove-like defect to occur in both SZ and TMAZ in addition to causing some pinholes which have been observed at the bottom side of the joint. The observed kissing bond has been formed under the pin shoulder during the FSW process due to the severities of the oxide with some absorbed air on the specimens' surface [9].

The optical micrograph of the welded sample at 900 rpm rotational speed and 35 mm/min traverse speed is shown in Figure 4. Despite the few microvoids observed in the SZ, it can be claimed that almost sound joints have been successfully produced by applying these levels of rotational and traverse

speeds. This is mainly because of the sufficient heat input applied during the FSW process which has elevated the temperature and promoted the plastic flow of materials around the pin tool in an effective manner.

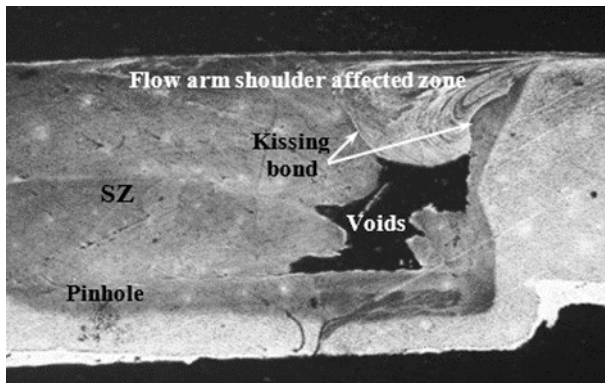


Fig. 3. A micrograph of the joints at 11 mm/min traverse speed and 900 rpm rotational speed.



Fig. 4. A micrograph of the joints at 35 mm/min traverse speed and 900 rpm rotational speed.

Optical micrograph of welded sample at 710 rpm rotational speed and 35 mm/min traverse speed is shown in Figure 5. As in the case of 900 rpm and 35 mm/min, few microvoids have been observed on the retreating side of SZ and TMAZ. The overall area percentage of the microvoids to the welding nugget is less than 1% indicating that the porosity level is still quite low. The cross-section of a typical FSW joint for the rotational speed of 1400 rpm and the traverse speed of 35 mm/min is shown in Figure 6. Voids have been obviously seen in the SZ and that could be attributed to the excess amount of heat generated by the high rotational speed of the pin tool. In addition, the excess heat input applied during the FSW has softened the metal and, as a result, has caused a large mass of flash to be ejected to the outside [22]. Figure 7 shows the ultimate tensile strength of the joints compared to the BM. Figure 7a presents the tensile strength of joints obtained at traverse speed of 35 mm/min and different rotational speeds, whereas part b of the figure presents the tensile strength of the joints obtained at rotational speed of 900 rpm and different traverse speeds. Both parts of this figure show that the tensile strength of the FSW joints is much lower than that of BM. The

stated findings agree with findings in [23]. From the experimental results shown in Figure 7a, the tensile strength of the joints has a tendency to increase when rotational speed increases until it reaches 900rpm. Rotational speeds higher than this value cause the tensile strength to decrease due to the higher temperatures experienced in the SZ. Of the five rotational speeds shown, 700 rpm and 900 rpm rotational speeds enhanced the tensile strength of the joints substantially but the other rotational speeds (560, 1400, and 1800 rpm) deteriorated tensile strength of the joints analyzed.

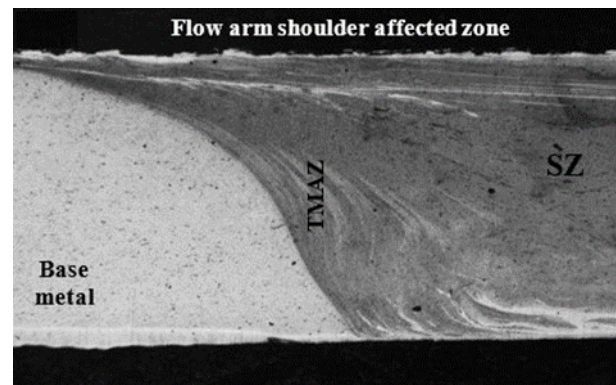


Fig. 5. A micrograph of the joints at 35 mm/min traverse speed and 700 rpm rotational speed.

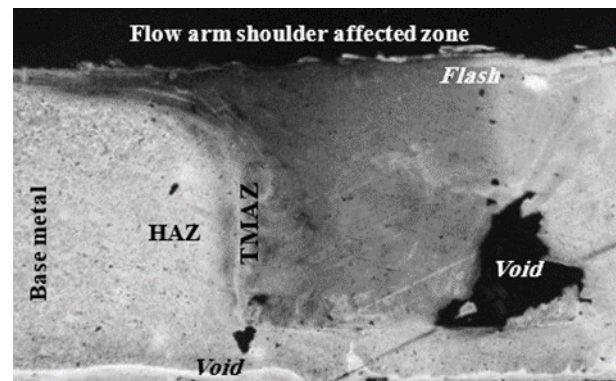


Fig. 6. A micrograph of the joints at 35 mm/min traverse speed and 1400 rpm rotational speed.

When varying the traverse speed at constant rotational speed (900rpm), as shown in Figure 7b, the tensile strength is decreased but with a magnitude lower than the one observed when varying the rotational speed at constant traverse speed. This coincides with findings in [24, 25] as they report that temperature and rotational speed are significantly affecting the strength and microstructure of joints. Figure 8 shows the tensile strength performances of the joints obtained at different rotational and traverse speeds. The strength performances are defined as the ratios of the tensile strength of the joints to those of the BM. The tensile strength performances of the joints vary with the welding condition. For the joints obtained at a traverse speed (35 mm/min) and different rotational speeds, the strength performances are varying between 54.9% at 560 rpm and 86.3% at 900 rpm. For the joints obtained at constant rotational

speed (900 rpm) and different traverse speeds, the strength performances are varying between 74.8% at 45 mm/min and 86.3% at 35 mm/min. The best results were obtained at a traverse speed of 35 mm/min for all tool rotational speeds.

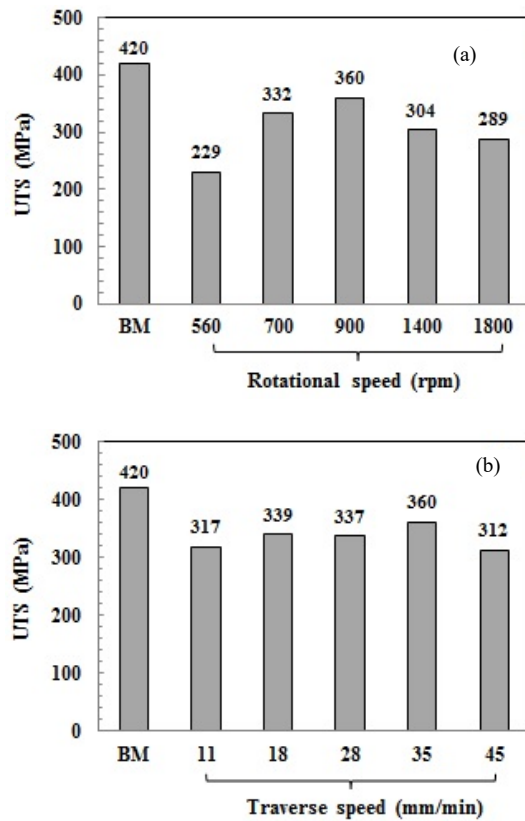


Fig. 7. Tensile strength of joints at different rotational and traverse speeds compared to BM. (a) at 35mm/min traverse speed and (b) at 900 rpm rotational speed.

Figure 9 shows the microhardness profiles across the weld cross-section of the FSW joints at 35 mm/min traverse speed and various rotational speeds. As illustrated, the BM in the initial condition has an average microhardness value of about 160 HV. This value is gradually decreasing in HAZ and TMAZ until it reaches its lowest level in the SZ. The minimum microhardness value observed in the SZ is 101 HV which is 63% of the BM value at 560 rpm rotational speed. Such reduction of the microhardness value within the welded zone is attributed to the softening of the welded zone caused by the excess heat input during joining. Similar microhardness behavior of other friction stir-joined Al alloys has also been reported by other researchers [3, 24, 26]. However, the effect of the excess heat generated during the FSW process on the microhardness level is highly affected by the rotational speed applied. The microhardness value has increased to 119 HV in the SZ at 700 rpm and to 117 HV at 900 rpm while it has decreased at 1400 and 1800 rpm rotational speeds. This reduction in the microhardness value at higher rotational speeds is due to grain growth resulting from higher temperatures experienced during the FSW process [27]. Such observation

coincides with findings in [21] which state that the rotational speed must be moderate enough to avoid grain growth.

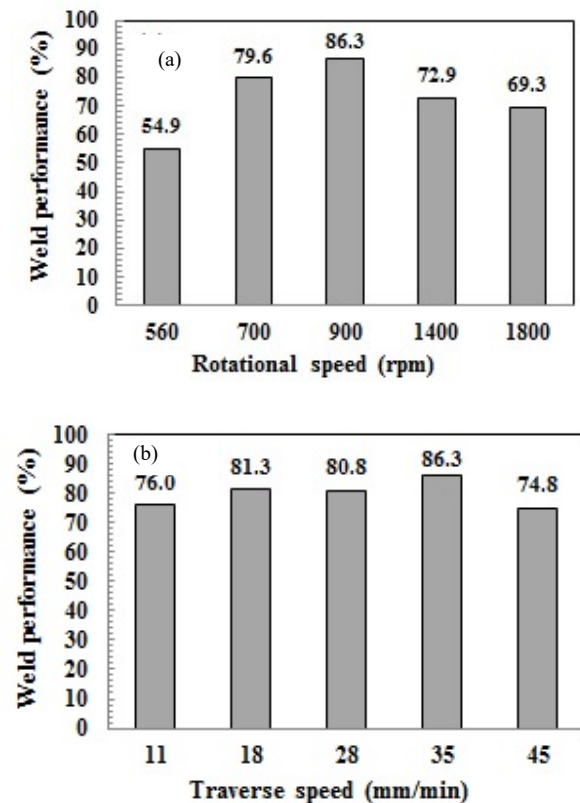


Fig. 8. Tensile strength performances of joints at (a) at 35mm/min, and (b) at 900 rpm.

Figure 10 shows the microhardness profiles across the weld cross-section of the FSW joints at 900 rpm rotational speed and two traverse speeds, 11 mm/min and 35 mm/min. As seen in the figure, the low traverse speed has decreased the microhardness value within the welded area by about 42.5% while the high traverse speed has decreased it by 26.8% of the BM microhardness value. With decreasing traverse speed, the time of exposure to the heat is increased and leads to grain growth. The mechanical resistance and the ductility of all joint specimens have been addressed using bending tests. These tests are very sensitive to defects near the surface of the welded zone. The welded specimens are loaded until they take a U-shape or a failure is observed. The bending tests were performed on the welded specimens obtained at different rotational and traverse speeds and the surface photographs of tested specimens are shown in Figure 11. As shown in Figure 11a, the welds presented good ductility, allowing for very high bend angles and no cracks or failures were observed on the welded specimens at the rotational speeds of 560, 700, and 900 rpm. On the other hand, cracks and failures are found in the welded zones on the specimens that have been welded at the rotational speeds of 1400 and 1800 rpm. The photographs of tested specimens in Figure 11b show that that the surface of most of the welded specimens seems to be good. Solely one specimen was observed to fail in the bend testing at the

traverse speed of 45 mm/min. Table III presents a summary of the conducted bend testing parameters and results

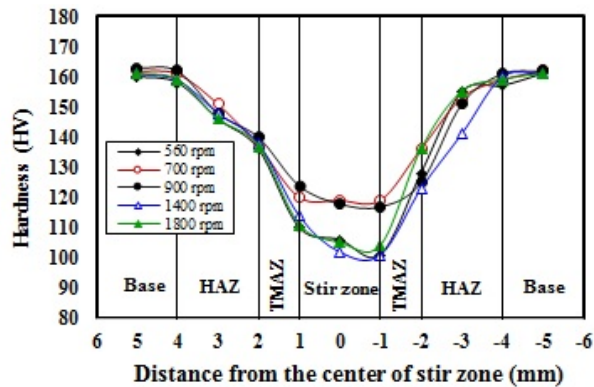


Fig. 9. Microhardness profile across the stirred zone at 35 mm/min traverse speed.

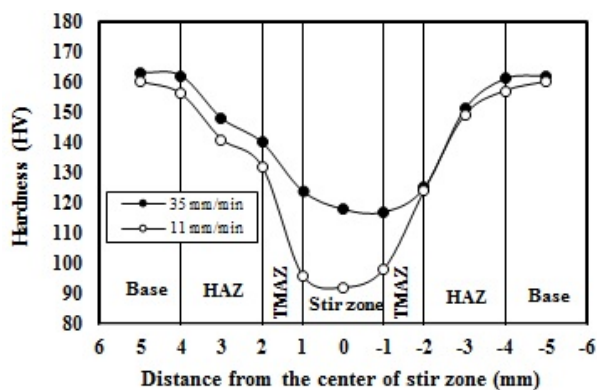


Fig. 10. Microhardness profile across the stirred zone at 900 rpm rotational speed and two different traverse speeds (11 mm/min and 35 mm/min).

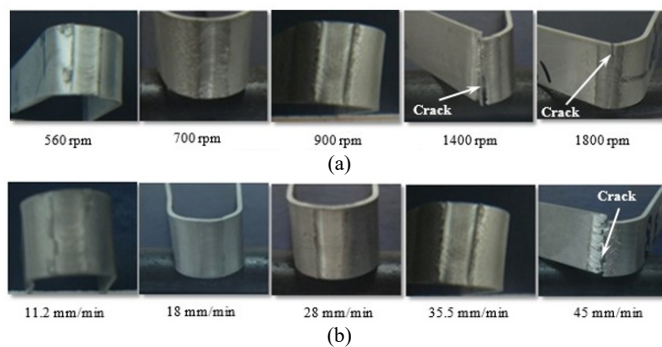


Fig. 11. The bending results of joints at different traverse and rotational speeds. (a) at 35mm/min and (b) at 900 rpm.

#### IV. CONCLUSIONS

In this study, the friction stir butt weldability of AA2024-T4 aluminum alloy was studied. The tensile, bending and microhardness tests, as well as microstructure analysis were conducted to determine the mechanical properties and the

welding performances of joints. The following conclusions were drawn:

- The almost sound joints were successfully produced at the rotational speeds of 900 rpm and 700 rpm and traverse speed of 35 mm/min. for the rotational speed of 1400 rpm.
- As a result of the tensile test it was observed that the maximum welding performance of joints was found to be 86.3% with a 900-rpm rotational speed and a 35 mm/min traverse speed. The tensile value is reached to 360 MPa in the welded sample. However, it is seen that the tensile strength values are decreased under the highest traverse speed (45 mm/min) and under the highest rotational speeds (1400 and 1800 rpm).
- The microhardness profile of all the welded sheets clearly shows a dramatic drop in microhardness measurements within the SZ. The hardness increases relatively quickly from the SZ through the HAZ toward the BM. The welded sheet at low traverse speed (11 mm/min) demonstrates a more abrupt microhardness value compared with the welded sheet at high traverse speed (35 mm/min).
- Most of the welds presented good ductility, allowing for very high bend angles and no cracks were observed.

TABLE III. EXPERIMENTAL BENDING RESULTS OF WELDED SAMPLES AT DIFFERENT TRAVERSE AND ROTATIONAL SPEEDS

Traverse speed (mm/min)	Rotational speed (rpm)	Remarks
35.5	560	No cracks
	710	No cracks
	900	No cracks
	1400	Cracks
	1800	Cracks
11.2	900	No cracks
18		No cracks
28		No cracks
35.5		No cracks
45		Cracks

#### REFERENCES

- [1] T. Dursun, C. Soutis, "Recent developments in advanced aircraft aluminium alloys", *Materials & Design*, Vol. 56, pp. 862–871, 2013
- [2] P. Kah, R. Rajan, J. Martikainen, R. Suoranta, "Investigation of weld defects in friction-stir welding and fusion welding of aluminium alloys", *International Journal of Mechanical and Materials Engineering*, Vol. 10, No. 1, p. 26, 2015
- [3] H. Aydın, A. Bayram, A. Uguz, S. Akay, "Tensile properties of friction stir welded joints of 2024 aluminum alloys in different heat-treated state", *Materials & Design*, Vol. 30, pp. 2211–2221, 2009
- [4] W. Xu, J. Liu, G. Luan, C. Dong, "Temperature evolution, microstructure and mechanical properties of friction stir welded thick 2219-O aluminum alloy joints", *Materials & Design*, Vol. 30, pp. 1886–1893, 2009
- [5] P. Cavaliere, R. Nobile, F. Panella, A. Squillace, "Mechanical and microstructural behaviour of 2024–7075 aluminium alloy sheets joined by friction stir welding", *International Journal of Machine Tools and Manufacture*, Vol. 46, No. 6, pp. 588–594, 2006
- [6] H. Aydın, A. Bayram, I. Durgun, "The effect of post-weld heat treatment on the mechanical properties of 2024-T4 friction stir-welded joints", *Materials & Design*, Vol. 31, pp. 2568–2577, 2010
- [7] J.-H. Cho, W. J. Kim, C. G. Lee, "Texture and microstructure evolution and mechanical properties during friction stir welding of extruded

- aluminum billets”, *Materials Science and Engineering: A*, Vol. 597, pp. 314–323, 2015
- [8] L. Karthikeyan, V. S. Senthilkumar, K. A. Padmanabhan, “On the role of process variables in the friction stir processing of cast aluminum A319 alloy”, *Materials & Design*, Vol. 31, pp. 761–771, 2010
- [9] J. Chen, R. Ueji, H. Fuji, “Double-sided friction-stir welding of magnesium alloy with concave-convex tools for texture control”, *Materials & Design*, Vol. 76, pp. 181–189, 2015
- [10] X. Cao, M. Jahazi, “Effect of welding speed on the quality of friction stir welded butt joints of a magnesium alloy”, *Materials & Design*, Vol. 30, pp. 2033–2042, 2009
- [11] S. Ji, Z. Li, Y. Wang, L. Ma, “Joint formation and mechanical properties of back heating assisted friction stir welded Ti–6Al–4V alloy”, *Materials & Design*, Vol. 113, pp. 37–46, 2017
- [12] K. Song, H. Fuji, K. Nakata, “Effect of welding speed on microstructural and mechanical properties of friction stir welded Inconel 600”, *Materials & Design*, Vol. 30, pp. 3972–3978, 2009
- [13] N. Xu, R. Ueji, Y. Morisada, H. Fuji, “Modification of mechanical properties of friction stir welded Cu joint by additional liquid CO<sub>2</sub> cooling”, *Materials & Design*, Vol. 56, pp. 20–25, 2014
- [14] H. Li, S. Yang, S. Zhang, B. Zhang, Z. Jiang, H. Feng, P. Han, J. Li, “Microstructure evolution and mechanical properties of friction stir welding super-austenitic stainless steel S32654”, *Materials & Design*, Vol. 118, pp. 207–217, 2017
- [15] M. Hajian, A. Abdollah-zadeh, S. Rezaei-Nejad, H. Assadi, S.M. Hadavi, K. Chung, M. Shokouhimehr, “Microstructure and mechanical properties of friction stir processed AISI 316L stainless steel”, *Materials & Design*, Vol. 67, pp. 82–94, 2015
- [16] P. Avinash, M. Manikandan, N. Arivazhagan, K.D. Ramkumar, S. Narayanan, “Friction Stir Welded Butt Joints of AA2024 T3 and AA7075 T6 Aluminum Alloys”, *Procedia Engineering*, Vol. 75, pp. 98–102, 2014
- [17] M. Ahmed, S. Ataya, M. E. Seleman, H. R. Ammar, E. Ahmed, “Friction stir welding of similar and dissimilar AA7075 and AA5083”, *Journal of Materials Processing Technology*, Vol. 242, pp. 77–91, 2017
- [18] C. Meran, O.E. Canyurt, “The effects of tool rotation speed and traverse speed on friction stir welding of AISI 304 austenitic stainless steel”, *International Journal of Materials Research*, Vol. 102, No. 4, pp. 420–428, 2011
- [19] ASTM E8 / E8M-13, *Standard Test Methods for Tension Testing of Metallic Materials*, ASTM International, West Conshohocken, PA, 2013
- [20] ASTM E190-14, *Standard Test Method for Guided Bend Test for Ductility of Welds*, ASTM International, West Conshohocken, PA, 2014, [www.astm.org](http://www.astm.org)
- [21] ASTM E290-14, *Standard Test Methods for Bend Testing of Material for Ductility*, ASTM International, West Conshohocken, PA, 2014, [www.astm.org](http://www.astm.org)
- [22] Y. G. Kim, H. Fuji, T. Tsumura, T. Komazaki, K. Nakata, “Three defect types in friction stir welding of aluminum die casting alloy”, *Materials Science and Engineering: A*, Vol. 415, pp. 250–254, 2006
- [23] K. Elangovan V. Balasubramanian, “Influences of post-weld heat treatment on tensile properties of friction stir-welded AA6061 aluminum alloy joints”, *Mater. Charact.*, Vol. 59, No. 9, pp. 1168–1177, 2008
- [24] L. Karthikeyan, V. Senthilkumar, V. Balasubramanian, S. Natarajan, “Mechanical property and microstructural changes during friction stir processing of cast aluminum 2285 alloy”, *Materials & Design*, Vol. 30, pp. 2237–2242, 2009
- [25] R. Palanivel, P. K. Mathews, N. Murugan, I. Dinaharan, “Effect of tool rotational speed and pin profile on microstructure and tensile strength of dissimilar friction stir welded AA5083-H111 and AA6351-T6 aluminum alloys”, *Materials & Design*, Vol. 40, pp. 7–16, 2012
- [26] P. Cavaliere P. P. DeMarco, “Friction stir processing of a Zr-modified 2014 aluminum alloy”, *Materials Science and Engineering: A*, Vol. 462, pp. 206–210, 2007
- [27] M. Azizieh, A. H. Kokabi, P. Abachi, “Effect of rotational speed and probe profile on microstructure and hardness of AZ31/Al<sub>2</sub>O<sub>3</sub> nanocomposites fabricated by friction stir processing”, *Materials & Design*, Vol. 32, pp. 2034–2041, 2011